멤브레인(Membrane Journal)
Vol.13, No.4 December, 2003, 239-245

은염을 포함하는 고분자 전해질 막을 통한 올레핀 촉진수송의 해석

고 동 균*,** · 김 종 학* · 정 성 택** · 강 용 수*†

*한국과학기술연구원 촉진수송분리막연구단, **인하대학교 화학공학
(2003년 9월 18일 접수, 2003년 11월 12일 채택)

Analysis of Facilitated Olefin Transport Through Polymer Electrolyte Membranes Containing Silver Salts

Dongkyun Ko*,, Jong Hak Kim*, Sung Taik Chung**, and Yong Soo Kang*†**

*Center for Facilitated Transport Membranes, KIST, Seoul
**Department of Chemical Engineering, Inha University, Incheon
(Received September 18, 2003, Accepted November 12, 2003)

요 약: 본 연구에서는 은-고분자 전해질 막에서의 프로필렌/프로판에 대한 순수 기체 선택도 (≈10,000)와 혼합기체 선택도 (≈40)의 큰 차이의 원인을 규명하였다. 먼저 기체 공급 조건이 혼합기체의 투과도와 분리 성능에 미치는 영향을 고찰하였다. 프로필렌의 농도가 감소함에 따라 고분자 전해질 막을 통한 프로필렌의 투과도는 감소하고, 프로판의 투과도는 증가를 하였으며, 그 결과 프로판/프로필렌의 선택도가 감소하였다. 이는 고분자 전해질막의 프로필렌에 의한 가소화에 의한 것임을 실험적 결과 및 수학적 모델에 의해서 확인하였다. 또한, 압력과 무관한 투과도를 사용하였을 때의 이론적 계산에 의한 막 분리 성능은 실험치와 비슷하게 나왔음을 알 수 있었다.

Abstract: The origin of large difference of selectivity of C_3H_6 over C_3H_8 between pure gas and mixed gas through silver polymer electrolyte membranes is investigated. Firstly, the effect of feed condition on the permeance of mixture gas (C_3H_6/C_3H_8) and the separation performance is examined. Upon decrease of the C_3H_6 concentration, the C_3H_6 permeance decreased whereas the permeance of C_3H_8 increased, resulting in the decrease of the selectivity of C_3H_6/C_3H_8. This result is ascribed to the C_3H_6-induced plasticization of membranes. Experimental results were validated by means of mathematical modeling, where pressure independent permeabilities were used.

Keywords: *membrane, facilitated transport, olefin, plasticization, mathematical model, orthogonal collocation on finite element method (OCFEM), gPROMS*

Introduction

Olefin/paraffin separation, one of the most important processes in petrochemical industry, has been typically performed by highly energy-intensive low-temperature distillation[1]. Among various alternative energy saving separation processes, the facilitated transport membranes employing silver polymer electrolytes have attracted significant interest because of their remarkable separation performance for olefin/paraffin in the solid state [2-15]. For example, when silver salts such as $AgBF_4$, $AgClO_4$, $AgSbF_6$ or $AgCF_3SO_3$ are dissolved in polymer matrices such as poly(2-ethyl-2-oxazoline) (POZ), poly(N-vinyl pyrrolidone) (PVP) or poly(ethylene oxide) (PEO), the silver ions are active as an olefin carrier, resulting in very high separation performance for olefin/paraffin mixtures. The C_3H_6 permeance increased up to almost 45 GPU at 140 kPa feed pressure with increasing silver ion content, while the C_3H_8 permeance decreased as low as 0.003 GPU[2,6]. Thus, the

†주저자(e-mail : yskang@kist.re.kr)

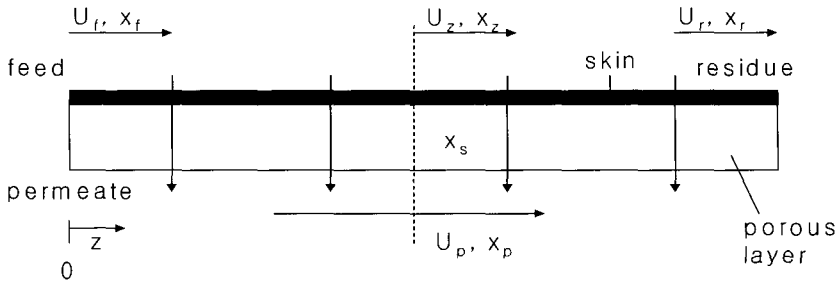

Fig. 1. Polymer electrolyte membrane. Feed pressure P_{feed} = 40 psi; Feed flow rate U_f = 1.8 cm^3/min; Feed mole fraction x_f = 0.5; Selectivity α = 10000.

ideal separation factor of C_3H_6 over C_3H_8 is more than 10,000. However, the selectivity for gas mixtures, defined by the ratio of mole fractions of the gas components in permeate and feed streams, is around 40[7]. Such a large difference of the selectivity between pure gas and mixed gas is considered to be due to the plasticization of membranes[5]. In an effort to investigate the possible effect of plasticization, we carried out the theoretical analysis of the effect of various feed conditions in the cocurrent permeation through silver polymer electrolyte membranes. The permeability and selectivity of membranes are assumed to be independent of the feed concentration and pressure, although they would be sensitive to the feed concentration for the real facilitated olefin transport membranes. A model for cocurrent single stage membrane and an orthogonal collocation on finite element method (OCFEM) in an external process simulator, gPROMS, based on the equation-oriented approach were developed to solve the differential model equations[16-21].

Experimental

Polymer electrolyte solutions containing equimolar amounts of $AgBF_4$ and a polymer were prepared by dissolving $AgBF_4$ (98%, Aldridh) in 20 wt% poly(2-ethyl-2-oxazoline) (POZ, M_w=5×10^5g/mol, Aldrich) in methanol. 2 wt% of dioctyl terephthalate (DOP, LG Chem. Co.) with respect to POZ was added to these solutions to prohibit the possible stability problem of membrane performance[22]. The solution was then coated onto polysulfone microporous membrane support (Seahan Industries Inc., Seoul, Korea) using an RK Control Coater (Model 101, Control Coater RK Print-Coat instruments LTD, UK). The solvent was evaporated in a light-protected convection oven at 25°C under a stream of nitrogen, and then the membrane was dried completely in a vacuum oven for 24 h at room temperature. The unit of the gas permeance is GPU, where 1 GPU = 1×10^{-6} cm^3 (STP)/(cm^2 s cmHg). Mixed gas (propylene:propane mixture) separation properties of the membranes were evaluated by gas chromatography (Hewlett Packard) equipped with a TCD and a unibead 2S 60/80 packed colum.

Solution Method

Partial differential and algebraic equations (PDAEs) are developed and solved using the gPROMS simulation software (Process Systems Enterprise Ltd). A spartial discretisation technique is employed for the solution of the distributed model. This converts the system of PDAEs into a set of ordinary DAEs, which can be solved by gPROMS using implicit numerical integration techniques[21].

Mathematical Model

For the mathematical formulation, the following assumptions are made similar to those of Weller and co-workers in membrane design[16-21]. Figure 1 shows the polymer electrolyte membrane, with feed flowing on the skin side and permeate stream.

1. The porous supporting layer has negligible resistance to the gas flow, and diffusion along the pore path is insignificant due to high permeate flux.
2. Feed gas pressure drop is negligible.
3. The deformation of the polymer electrolyte membrane is negligible.
4. The permeability and permselectivity are constant.
5. Steady-state operation.
6. The permeate mole fraction is constant.
7. The concentration of the permeate leaving the membrane skin surface, x_s, is generally different from that of the bulk permeate stream outside the porous layer, x_p, except at the closed end of the membrane where x_s, x_p, are identical.

The permeation and transport of gases through a differential element of the membrane at length z are described by the following set of differential equations [16-20]:

Permeate side of the propylene

$$\frac{d(F_z x_z)}{dz} = -LQ_{py}(P_{feed}x_z - P_{permeate}x_s) \tag{1}$$

Permeate side of the propane

$$\frac{d(F_z(1-x_z))}{dz} = -LQ_{pa}(P_{feed}(1-x_z) - P_{permeate}(1-x_s)) \tag{2}$$

Local material balance

$$\frac{d(F_z x_z)}{dz} = x_s \tag{3}$$

Overall material balances

$$F_z = F_p + F_r \tag{4}$$

$$F_z x_z = F_p x_p + F_r x_r \tag{5}$$

The porous path mole fraction x_s is obtained with the aid of Eq. (3) and ratio of Eqs. (1) and (2):

$$x_s = \frac{1+(\alpha-1)(\gamma+x_z) - \sqrt{[1+(\alpha-1)(\gamma+x_z)]^2 - 4\gamma(\alpha-1)\alpha x_z}}{2\gamma(\alpha-1)} \tag{6}$$

The sum of Eqs. (1) and (2) with the aid of Eqs. (3), (5) and (6) becomes:

$$\frac{dx_z}{d_z} = LQ_{pa}\frac{P_{feed}}{F_f} \frac{(x_z-x_p)(x_s-x_z)[\alpha(x_z-\gamma x_s)+(1-x_z)-\gamma(1-x_s)]}{(x_p-x_f)} \tag{7}$$

$$\frac{dx_p}{d_z} = LQ_{pa}\frac{P_{feed}}{F_f} \frac{(x_z-x_p)(x_p-x_s)[\alpha(x_z-\gamma x_s)+(1-x_z)-\gamma(1-x_s)]}{(x_f-x_z)} \tag{8}$$

Boundary conditions

$$z = 0 : x_p = x_{sf}\ x_z = x_f \tag{9}$$

Results and Discussion

In order to analyze the efficiency of the permeators, the permeate concentration and the residue concentration were plotted against the real length for various feed conditions such as feed flow rate, feed pressure and feed concentration. The simulations were performed for binary gas mixtures containing C_3H_6 and C_3H_8.

Figure 2 shows the effect of feed flow rate (U_f) on membrane performance with the ideal separation factor of 10000, propylene permeance (Q_{py}) of 15 GPU, propane permeance (Q_{pa}) of 1.5×10^{-3} GPU and the feed pressure of 40 psi and the various feed flow rate. It is found that both the permeate and the residue concentrations are strongly dependent on the values of feed flow rate. Especially, the permeate and residue concentrations decreased more sharply when the feed flow rate was low. Figure 3 presents the permeate concentration dependency on feed pressure. The permeate concentration decreased with increasing feed pressure up to 0.08 m of membrane length more drastically at low feed pressure than at high pressure. Thus the crossover of the permeate concentration occurs at 0.08 m of the membrane length. Therefore, the membrane length should be optimized depending on the feed condition.

Figure 4 shows the effect of feed concentration on

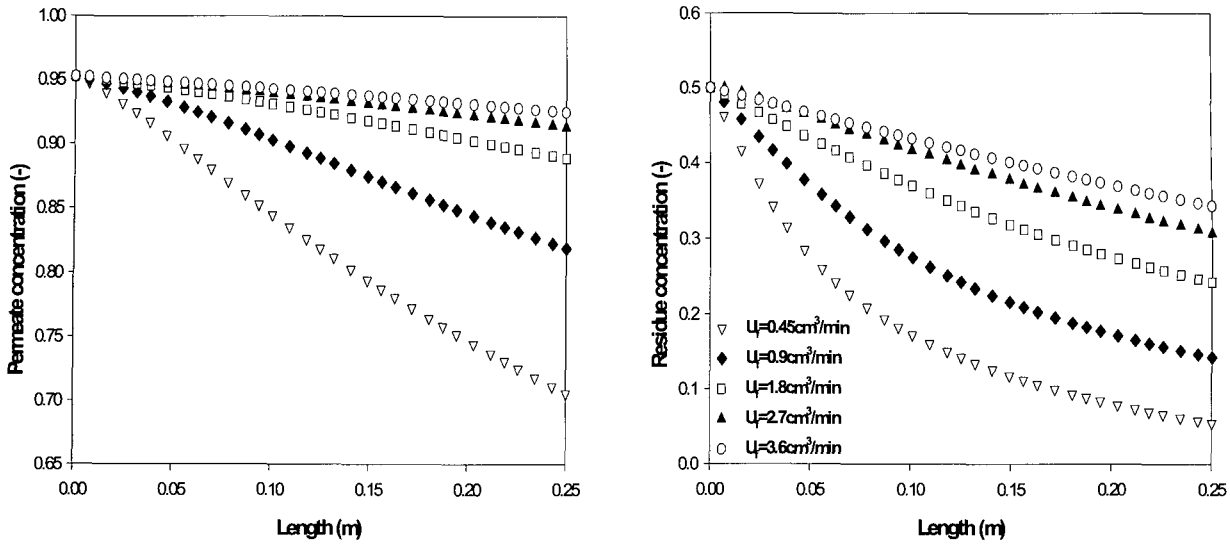

(a) (b)

Fig. 2. Effect of feed flow rate (U_f) on (a) permeate concentration and (b) residue concentration as a function of membrane length. Feed pressure P_{feed} = 40 psi; Feed mole fraction x_f = 0.5; Selectivity α = 10000.

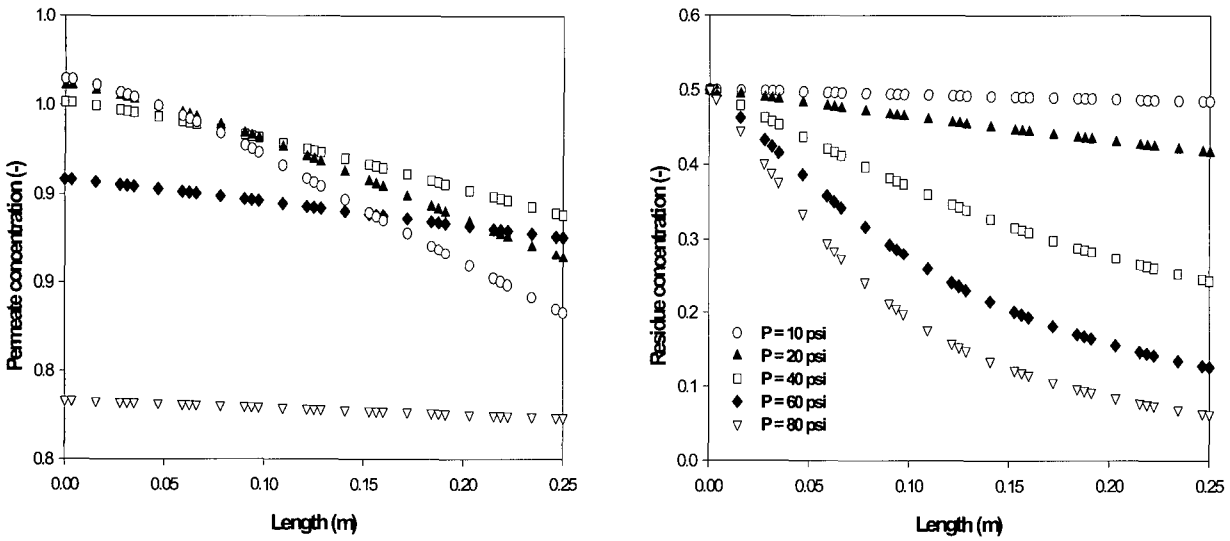

(a) (b)

Fig. 3. Effect of various feed pressure (P) on (a) permeate concentration and (b) residue concentration as a function of the membrane length. Feed flow rate U_f = 1.8cm³/min; Feed mole fraction x_f = 0.5; Selectivity α = 10000.

permeate and residue concentrations. These data were obtained from the assumption that the membrane permeabilities and the selectivities are independent of feed pressure and feed concentration. Thus, one of the reasons for the large selectivity difference between pure gas and mixed gas would be due to the property changes of membrane by plasticization. Similar C_3H_6-induced plasticization of silver polymer electrolyte membranes is observed by the FT-Raman spectroscopy [5]. Figure 5 presents the permeate concentration of C_3H_6 and C_3H_8 and the selectivity of C_3H_6/C_3H_8, obtained by varying the feed composition. The permeate concentration of C_3H_6 decreased whereas that of C_3H_8 increased with the decrease of C_3H_6 concentration,

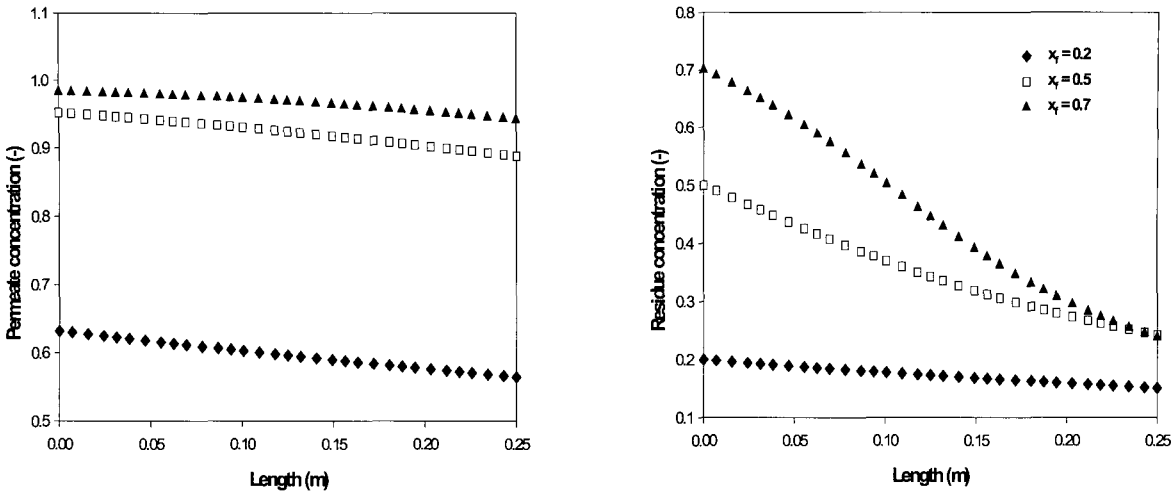

(a) (b)

Fig. 4. Effect of various feed concentration (x_f) on (a) permeate concentration and (b) residue concentration as a function of the membrane length. Feed flow rate U_f = 1.8cm^3/min; Feed pressure P_{feed} = 40 psi; Selectivity α = 10000.

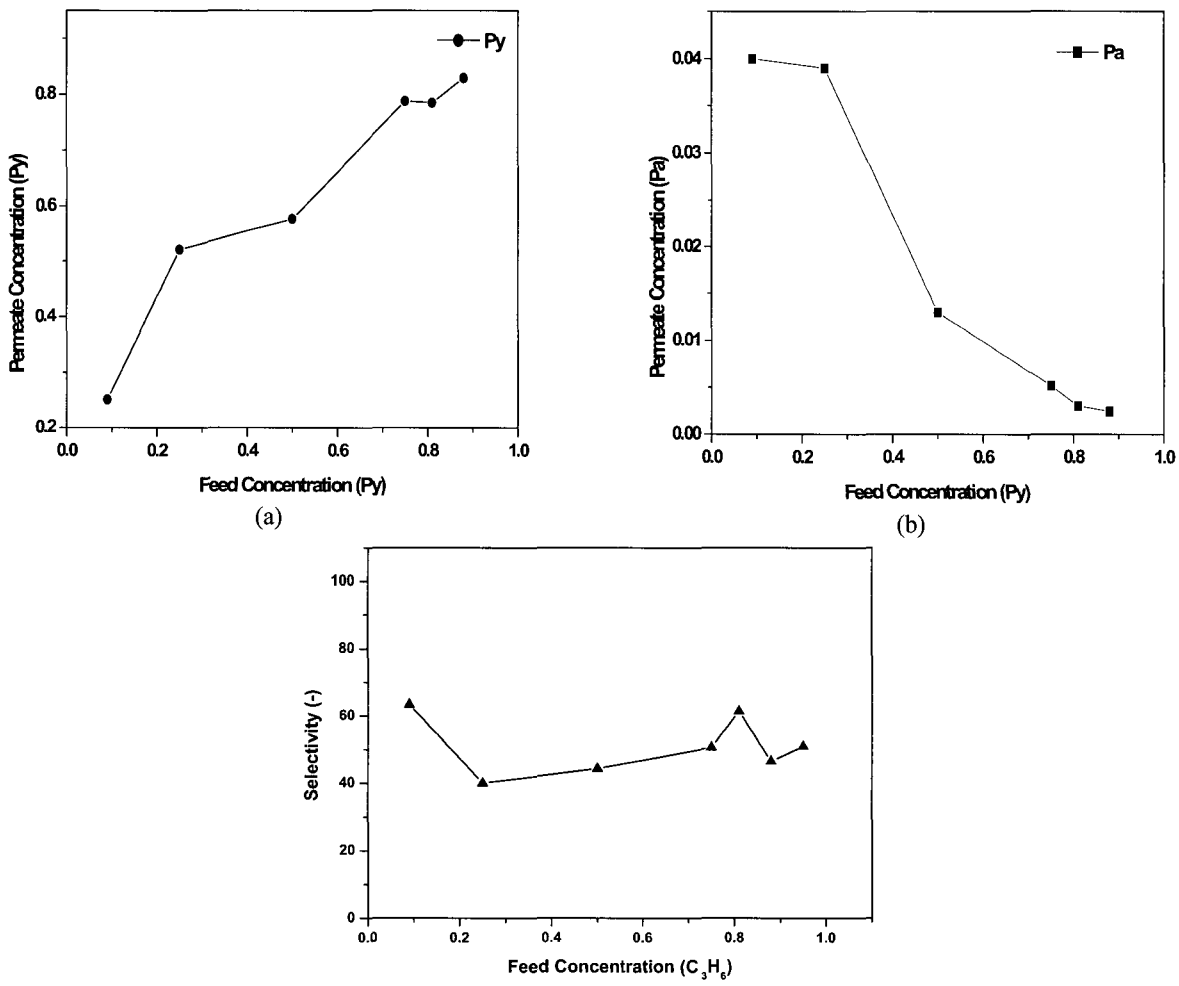

(a) (b) (c)

Fig. 5. The experimental permeate concentration and selectiviy of (a) C_3H_6, (b) C_3H_8 and (c) selectivity by varying the feed composition.

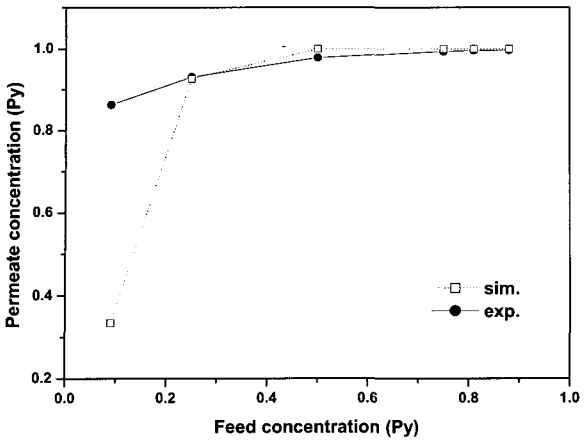

Fig. 6. The comparison between experimental results and simulation predictions in terms of C_3H_6 permeate concentrations. Feed flow rate U_f = 1.8cm^3/min; Feed pressure P_{feed} = 40 psi; Feed mole fraction x_f = 0.5; Selectivity α = 10000.

leading to the decrease of C_3H_6/C_3H_8 selectivity. Figure 6 shows the comparison between the experimental data and simulation results. When the experimental gas permeances obtained from the pure gas are used in the mathematical model, the simulated concentration values are in good agreement with the experimental values above 25% of C_3H_6 in the mixture, but they deviate significantly below 25% of C_3H_6. This would be due to the theoretical calculation by using concentration independent permeability and selectivity. Therefore, the measurement of concentration dependent permeability and selectivity is under way experimentally by varying the feed composition. From these data, we will investigate the origin of the large difference of selectivity between pure gas and mixed gas to obtain more exact result.

Conclusion

The C_3H_6 permeance through the facilitated olefin transport membranes employing silver polymer electrolyte increased with the increase the C_3H_6 concentrations, whereas the C_3H_6 permeane decreased, resulting in the decrease of the selectivity of C_3H_6/C_3H_8. The selectivity of pure gas through silver polymer electrolyte membranes is very high ($C_3H_6/C_3H_8 \approx 10000$), but the mixed gas selectivity is relatively low ($C_3H_6/C_3H_8 \approx 40$). These results would be due to the membrane plasticization by C_3H_6 gas, which was confirmed by numerical calculation using an external process simulator, gPROMS. Experimental and simulation results are in good agreement when the C_3H_6 concentration in the feed is higher than 25%.

Acknowledgement

This research was supported by the Ministry of Science and Technology of Korea through the Creative Research Initiatives Program (YSK) and INHA UNIVERSITY Research Grant (INHA-30202) (STC).

Nomenclature

F	flow rate, mol/s
L	membrane length, m
P	pressure, Pa
Q	permeability, mol/m s Pa
x	concentration, mole fraction
z	membrane length variable in orthogonal collocation procedure
α	ideal separation factor

Subscripts

f	feed
p	permeate side
py	propylene
pa	propane
permeate	permeate side
feed	feed side
r	residue final
s	local permeate side on the membrane surface

References

1. R. B. Eldridge, "Olefin/paraffin separation technology: A Review" *Ind. Eng. Chem. Res.*, **32**, 2208 (1993).

2. S. U. Hong, J. Won, and Y. S. Kang, "Polymer-salt complexes containing silver ions and their application to facilitated olefin transport membranes", *Adv. Mater.*, **12**, 968 (2000).
3. J. H. Kim, B. R. Min, C. K. Kim, J. Won, and Y. S. Kang, Role of transient cross-links for transport properties in silver-polymer electrolytes, *Macromolecules* 34,6052 (2001).
4. J. H. Kim, B. R. Min, C. K. Kim, J. Won, and Y. S. Kang, Spectroscopic interpretation of silver ion complexation with propylene in silver polymer electrolytes, *J. Phys. Chem. B.* 106, 2786 (2002).
5. J. H. Kim, B. R. Min, J. Won, and Y. S. Kang, Complexation Mechanism of Olefin with Silver Ions Dissolved in Polymer Matrix and its Effect on Facilitated Olefin Transport, *Chem. Eur. J.* **8**, 650 (2002).
6. J. H. Kim. B. R. Min, C. K. Kim, J. Won, and Y. S. Kang, New Insights into the Coordination Mode of Silver Ions Dissolved in poly(2-ethyl-2-oxazoline) and its relation to facilitated olefin transport, *Macromolecules* **35**, 5250 (2002).
7. J. H. Kim. B. R. Min, J. Won, S. H. Joo, H. S. Kim, and Y. S. Kang, Role of PolymerMatrix in Polymer/Silver Complexes for Structure, Interactions and Facilitated Olefin Transport, *Macromolecules* **36**, 6183 (2003).
8. J. H. Kim, B. R. Min, C. K. Kim, J. Won, and Y. S. Kang, Ionic interaction behavior and facilitated olefin transport in PVP:AgCF3SO3 electrolytes; Effect of molecular weight, *J. Poly. Sci. B. Poly. Phys.* **40**, 1813 (2002).
9. J. H. Kim, B. R. Min, K. B. Lee, J. Won, and Y. S. Kang, Coordination Structure of Various Ligands in Crosslinked PVA to Silver Ions for Facilitated Olefin Transport, *Chem. Commun.* 2732 (2002).
10. J. H. Kim, B. R. Min, H. S. Kim, J. Won, and Y. S. Kang, Facilitated transport of ethylene across polymer membranes containing silver salt: effect of HBF_4 on the photoreduction of silver ions, *J. Membr. Sci.* **212**, 283 (2003).
11. J. H. Kim, B. R. Min, J. Won, and Y. S. Kang, Revelation of Facilitated Olefin Transport through Silver-Polymer Complex Membranes using Anion Complexation, *Macromolecules* **36**, 4577 (2003).
12. I. Pinnau, L. G. Toy, and C. Casillas, Olefin separation membrane and process, *U. S. Patent* 5,670,051 (1997).
13. S. Sunderrajan, B. D. Freeman, C. K. Hall, and I. Pinnau, Propane and propylene sorption in solid polymer elelctrolytes based on poly(ethylene oxide) and silver salts, *J. Membr. Sci.* **182**, 1 (2001).
14. I. Pinnau and L. G. Toy, Solid polymer electrolyte composite membranes for olefin/paraffin separation, *J. Membr. Sci.* **184**, 39 (2001).
15. T. C. Merkel, Z. He, A. Morisato, I. Pinnau, Olefin/paraffin solubility in a solid polymer electrolyte membrane, *Chem. Commun.* 1596 (2003).
16. S. Weller, W. A. Steiner, Separation of gases by fractional permeation through membranes *J. Appl. Phys.* **21**, 279 (1950).
17. S. Weller and W. A. Steiner, Engineering aspects of separation of gases *Chem. Eng. Prog.* **46**, 585 (1950).
18. C. Y.Pan, Gas separation by permeators with high-flux asymmetric membranes, *AIChE J.* **29**, 545 (1983).
19. S. W Smith., C. K. Hall, B. D. Freeman, and R. Rautenbach, Corrections for analytical gas-permeation models for separation of binary gas mixtures using membrane modules *J. Memb. Sci.* **118**, 289 (1996).
20. S. P. Kaldis, G. C. Kapantaidakis, and T. I. Papadopoulos, G. P. Sakellaropoulos, Simulation of binary gas separation in hollow fiber asymmetric membranes by orthogonal collocation *J. Memb. Sci.* **142**, 43 (1998).
21. J. I. Marriott, E. Sorensen, and I. D. L. Bogle, Detailed mathematical modelling of membrane modules *Comp. & Chem. Eng.* **25**, 693 (2001).
22. B. Jose, J. H. Ryu, Y. J. Kim, H. Kim, Y. S. Kang, S. D. Lee, and H. S. Kim, Effect of plasticizers on the formation of silver nanoparticles in polymer electrolyte membranes for olefin/paraffin separation *Chem. Mater.* **14**, 2134 (2002).